CHEMICAL ENGINEERING TRANSACTIONS
VOL. 117, 2025
A publication of AIDIC
The Italian Association of Chemical Engineering
Online at www.cetjournal.it
Guest Editors: Fabrizio Bezzo, Flavio Manenti, Gabriele Pannocchia, Almerinda di Benedetto

ISBN 979-12-81206-17-5; **ISSN** 2283-9216
DOI: 10.3303/CET25117123

Activation of Dinitrogen Molecule (N_2) in Unconventional Electrochemical Reactors for Ammonia Production

Matteo Miceli*, Francesco Tavella, Daniele Giusi, Muluken Eshetu Tefera, Marco Francesco Torre, Siglinda Perathoner, Gabriele Centi, Claudio Ampelli

Department of Chemical, Biological, Pharmaceutical and Environmental Sciences (ChiBioFarAm) – University of Messina, ERIC aisbl and CASPE/INSTM, v.le F. Stagno d'Alcontres, 31 – 98166 Messina, Italy
matmiceli@unime.it

In this study, we present the development of a novel electrochemical device designed for the nitrogen reduction reaction (NRR) process, which operates under unconventional conditions. This zero-gap flow cell works without a liquid electrolyte in the cathodic section and incorporates novel electrocatalysts integrated into gas diffusion electrodes (GDEs). Specifically, the electrocatalysts are based on ruthenium (Ru), deposited on alumina (Al_2O_3) or carbon nanotubes (CNTs). A key objective of this study is to evaluate the partial or total replacement of Ru with a more abundant and cost-effective material, such as iron (Fe). The productivity of the produced NH_3 (in $\mu g\ mg_{cat}^{-1}\ h^{-1}$) and the Faradaic Efficiency (FE) are provided and discussed. Another important aspect of this work is how ammonia contamination is addressed, using a cheaper but still rigorous protocol than the one reported in the literature using expensive labelled nitrogen (N^{15}). Results show that cell design plays a key role, and the partial substitution of an abundant material (Fe) brings benefits, compared with the common noble metals reported in the literature. Furthermore, this contribution identifies the critical aspects to be addressed, emphasizing the need for breakthroughs to enhance performance in this highly challenging process.

1. Introduction

Nitrogen reduction reaction (NRR) is a today's challenge to meet the growing demand for ammonia. The Haber Bosh process is the only current industrial-scale ammonia production system, operating at high pressures and temperatures (20−40 MPa, 400−600 °C). This process is highly energy intensive as it consumes 1% of global energy production (Schrock, 2006) and emits millions of tons of CO_2 into the atmosphere (Rafiqul et al., 2005) despite the Haber Bosh reactor and the process itself being highly engineered and optimized (Rowenhorst et al., 2021). For this reason, the challenge is to find an emerging technology that allows ammonia to be obtained in a more sustainable and decentralized way. Among the various innovative approaches to ammonia production, there are electrocatalytic processes that exploit electrical energy to drive the reactions and can be perfectly integrated with the current energy transition, although the electrocatalysis remains far from industrial standards (Tavella et al., 2022). The main problems of electrochemical NRR are the low solubility of nitrogen in the aqueous medium and the concurrent hydrogen evolution reaction (HER).
Reactors that operate without electrolyte have recently attracted attention. This work aims to compare the performance of noble and non-noble metals when processed in these innovative gas-phase electrochemical devices. Ruthenium (Ru) and Iron (Fe) are found at the top of the volcano plot (Guo et al., 2019) and therefore have a greater affinity for the dinitrogen molecule, whose triple bond (945 kJ mol^{-1}) is difficult to break (Li et al., 2022). In the literature, many works use CNTs as conductive supports specially doped with nanoparticles (Chen et al., 2017), such as Fe_2O_3 or Ru, while metal doped α-alumina has been mainly reported for thermal catalysis and plasma catalysis, but less for electrocatalysis.
Numerous studies highlight how the analysis protocol is important to avoid false positives in the detection of ammonium ion in relation to the low productivity in water and the numerous sources of contamination. For this reason, the most rigorous protocols foresee high analysis costs for the use of labelled nitrogen, but this is

Paper Received: 11 January 2025; Revised: 10 April 2025; Accepted: 11 May 2025
Please cite this article as: Miceli M., Tavella F., Giusi D., Tefera M.E., Torre M.F., Perathoner S., Centi G., Ampelli C., 2025, Activation of Dinitrogen Molecule (N2) in Unconventional Electrochemical Reactors for Ammonia Production , Chemical Engineering Transactions, 117, 733-738 DOI:10.3303/CET25117123

unsustainable for research purposes. A new protocol is also discussed, offering improved cost-effectiveness and ease of use while maintaining a high degree of rigor.
To achieve gas-phase conditions (also known as electrolyte-less or zero-gap conditions), a membrane electrode assembly (MEA) can be used, similar to fuel cell technology (Ampelli, 2020). The MEA involves coupling the catalyst with an ion-exchange membrane to create a solid electrolyte, replacing the liquid cathodic compartment (Park et al., 2023). Factors such as i) increased N_2 concentration on the electrode surface and ii) regulated proton mobility in the catalyst/membrane interface enable catalytic surface reactions to form ammonia while limiting hydrogen (H_2) generation. Engineering the electrochemical reactor and related electrodes can lead to drastic changes in selectivity and a decrease of H_2 production as a side reaction. Specifically, this depends on mass and charge transfer phenomena at the electrode interface. In this view, the performance of different catalysts doped with noble metals are compared and the total or partial replacement with more abundant metals will be compared. This configuration, in addition to allowing a continuous supply of nitrogen species onto the electrocatalytic surface, has the advantage of i) allowing to design compact and scalable systems to an industrial level; ii) limiting the diffusion processes present in the liquid phase and iii) easy recovery of the liquid products.

2. Experimental

2.1 Al_2O_3-based catalysts preparation

Blank α-alumina pellets (MaTeck) with a surface area of 0.18 $m^2\ g^{-1}$ were purchased, smashed, and separated by mechanical milling and sieving in the range of 250-355 μm.

2.1.1 Ru/Al_2O_3

The α-alumina (0.95 g) and Ruthenium(III) chloride hydrate (0.1316 g, $RuCl_3{\cdot}xH_2O$, Ru basis, 38.0-42.0%) were used to make an aqueous suspension (25 mL ultrapure H_2O) for the wet impregnation process. After one hour of impregnation, the sample was dried overnight and then calcined in air at 400 °C for 4 h, and finally reduced at 400 °C in a tubular furnace under H_2 and Ar flow for 4 h. A metal loading of 5 wt.% Ru/Al_2O_3 was obtained.

2.1.2 $Ru\text{-}Fe/Al_2O_3$

The α-alumina (1.90 g), Ruthenium(III) chloride hydrate (0.256 g, $RuCl_3{\cdot}xH_2O$, Ru basis, 38.0-42.0%) and iron(III) nitrate nonahydrate (0.361 g, $Fe(NO_3)_3{\cdot}9H_2O$, ≥ 99.95% trace metals basis) were used to make an aqueous suspension (25 mL ultrapure H_2O) for the wet impregnation process. After one hour of impregnation, the sample was dried overnight, then calcined in air at 400 °C for 4 h, and finally reduced at 400 °C in a tubular furnace under H_2 and Ar flow for 4 h. The final metal loading of $Ru\text{-}Fe/Al_2O_3$ was 2.5 wt.% for iron and 2.5 wt.% for ruthenium.

2.1.3 Fe_2O_3/Al_2O_3

The α-alumina (0.903 g) and Fe-precursor, iron(III) nitrate nonahydrate (0.253 g, $Fe(NO_3)3{\cdot}9H_2O$, ≥ 99.95% trace metals basis), were suspended in 25 mL of deionized water with 1 mL of Ethylene Glycol; then, the mixture was sonicated for 30 minutes, and the pH was adjusted to 8 with a 5% ammonium hydroxide solution. Afterwards, the solvent was eliminated by drying at 120 °C overnight. The obtained powder was calcined for 2 h at 400°C in a horizontal tubular furnace under Ar flow. A metal loading of 5 wt.% was finally obtained.

2.2 CNTs-based catalysts preparation

The functionalization of CNTs consists of a pre-treatment of commercial CNTs (Pyrograph-III, PR-24XT) with Nitric Acid (conc. 65%), 50 mL for 1 g of CNTs, in order to create oxygen functionalities as reported by Hirsh, A. and Volstrowsky, O. (2005), hereafter called CNTs for simplicity, then treated at 120 °C for 2 h in a reflux apparatus (Chen et al., 2020). The suspension was filtered and washed with deionized water until neutral pH. The sample was dried at 80°C overnight.

2.2.1 Ru/CNTs

The CNTs (0.425 g) and Ru-precursor, Ruthenium(III) chloride hydrate (0.128 g, $RuCl_3{\cdot}xH_2O$, Ru basis, 38.0-42.0%) were dissolved in 25 mL of deionized water, then the mixture was stirred for 1.5h. Afterwards, the solvent was eliminated by drying at 120 °C overnight. The obtained powder was calcined for 4 h at 400°C in a horizontal tubular furnace under H_2 and Ar flows. The Ru-CNTs sample was obtained with a final metal loading of 5 wt.%.

2.2.2 Ru-Fe/CNTs

The CNTs (0.95 g) and Ru-precursor, Ruthenium(III) chloride hydrate (0.180 g, $RuCl_3 \cdot xH_2O$, Ru basis, 35.0-40.0%) and iron(III) chloride hexahydrate (0.121 g, $FeCl_3 \cdot 6H_2O$) were dissolved in 25 mL of deionized water, then the mixture was stirred for 1.5 h. Afterwards, the solvent was eliminated by drying at 120 °C overnight. The obtained powder was calcined for 4 h at 400°C in a horizontal tubular furnace under H_2 and Ar flows. The Ru-Fe/CNTs was finally obtained with 2.5 wt.% iron and 2.5 wt.% ruthenium.

2.2.3 Fe_2O_3/CNTs

The CNTs (0.7 g) and Fe-precursor, Iron(III) nitrate nonahydrate (1.515 g, $Fe(NO_3)_3 \cdot 9H_2O$, ≥ 99.95% trace metals basis), were dissolved in 25 mL of deionized water with 1 mL of Ethylene Glycol, then the mixture was sonicated for 30 minutes, and the pH was adjusted to 8 with a 5% ammonium hydroxide solution. Afterward, the solvent was eliminated by drying at 120 °C overnight. The obtained powder was calcined for 2 h at 400°C in a horizontal tubular furnace under He flows. The Fe_2O_3-CNTs was finally obtained with 30 wt.% metal loading.

2.3 Electrode preparation

In the electrode fabrication process, a commercial gas-diffusion layer (GDL), specifically the Sigracet GDL 39BB, and a Nafion® membrane N115 were provided by SGL Group, and a 10 wt.% weight Nafion solution used. The ink preparation consisted in a sonication of 50 mg of catalyst, 8 mL of isopropanol, and 50 μL of a perfluorinated (10 wt.%) Nafion solution, for 30 minutes until a uniform and homogeneous mixture was attained. Subsequently, the prepared ink was applied via spray coating and deposited across a 25 cm^2 area. Once the load is reached, the catalyst is cut into a round shape (20 mm diameter) and hot-pressed for 15 s at 130°C with a purified Nafion membrane (Membrane Electrode Assembly - MEA). All the chemical reagents used in this study were of analytical grade without any purification.

2.4 Electrochemical device

The electrocatalytic tests were conducted using a gas-phase cell reactor (refer to Figure 1). The flow reactor operates under room temperature and atmospheric pressure. The gas-phase reactor consists of i) a cathode compartment made of a gas-chamber in which the N_2 flows through the GDL, ii) the deposited catalyst and iii) the proton-exchange membrane (Nafion®115), assembled to form the MEA (see Figure 1) to form the working electrode (WE). The N_2 adsorbs on the catalyst surface and reacts with the protons diffusing from the proton-exchange membrane (Tavella et al., 2022). The membrane guarantees separation with the anodic compartment filled with N_2-saturated Na_2SO_4 aqueous solution, in which a commercial Pt electrode acts as a counter electrode (CE) and Ag/AgCl (3.0M KCl) electrode as the reference (RE). The gas products diffuse back into the gas chamber and are absorbed in a dilute solution of sulfuric acid (0.001 M) that acts as a trap for the produced NH_3. At the end of the test, the trap solution was analysed using the Ion Chromatography (IC, cationic column), and the electrolyte was analysed using the Salicylic method (UV-Vis, Jasco 570).

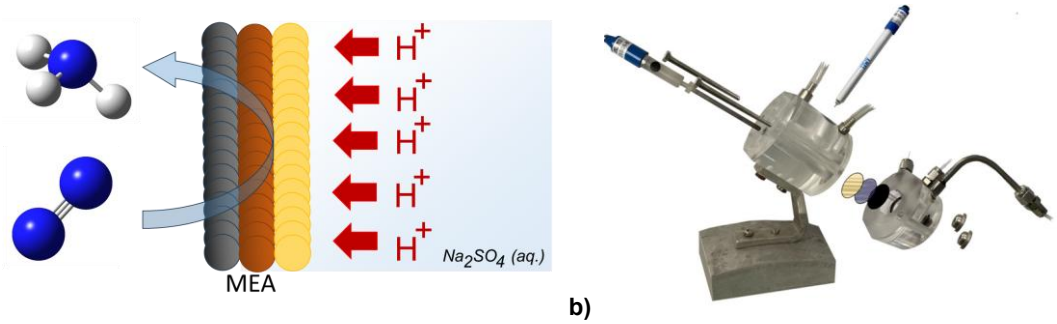

Figure 1: a) Gas-phase assembly. Black, orange, and yellow circles refer to GDL, catalyst, and membrane, respectively, and b) exploded depiction of the cell.

3. Results and Discussion

3.1 X-Ray diffraction (XRD) analysis

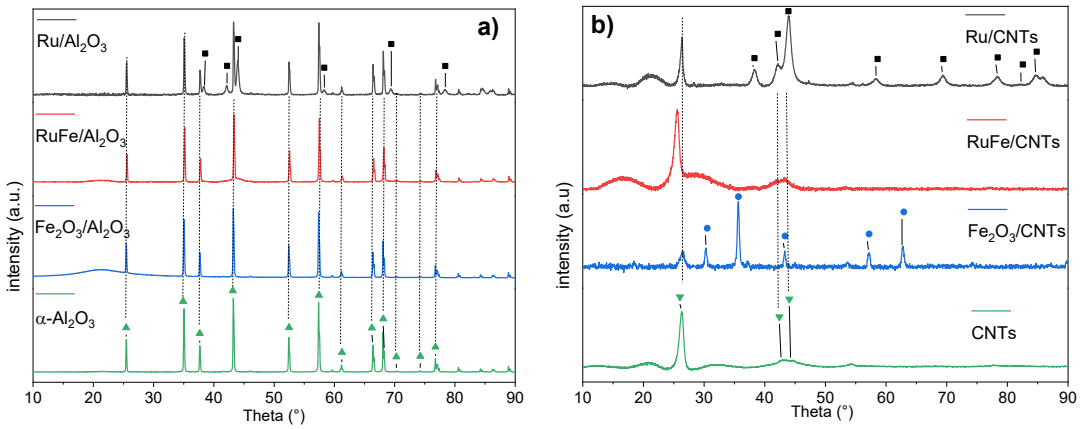

Figure 2: XRD patterns for a) Al_2O_3-based catalysts and b) CNTs-based catalysts. In figure (■) Ruthenium, (●)Fe_2O_3, (▲) Al_2O_3 and (▼) CNTs respectively.

Figure 2a shows the Alumina-based catalysts. The diffraction peaks at 2Θ =25.58, 35.16, 37.78, 43.36, 52.56, 57.51, 59.75, 61.32, 66.53, 68.22, 70.43, 74.32, 76.89, 77.25 are related to α-Al_2O_3 (International Center of Diffraction Data -ICDD- of card number 00–010–0173 of α- Al_2O_3) corresponding to the (0 1 2), (1 0 4), (1 1 0), (1 1 3), (0 2 4), (1 1 6), (2 1 1), (0 1 8), (2 1 4), (3 0 0), (1 2 5), (2 0 8), (1 0 10) and (1 1 9) planes, respectively (green line in Figure 2a). Diffraction peaks at 2Θ = 38.41, 42.18, 44.04, 58.36, 69.47, 78.41, for Ruthenium (JCPDS card no. 89-3942) correspond to the (1 0 0), (0 0 2), (1 0 1), (1 0 2), (1 1 0) and (1 0 3) planes, respectively (black line in Figure 2a). Fe_2O_3 and Ru-Fe are not detectable from XRD but are confirmed by Energy Dispersive X-ray (EDX) analysis. Figure 2b, shows the CNTs-based catalyst. CNTs characteristic peaks at 2Θ = 26, 42, and 48 are related to (0 0 2), (1 0 0), and (1 0 1) planes, respectively. For Fe_2O_3, it can be observed the peaks at 2Θ =30.3, 35.6, 43.3, 53.8, 57.1 and 62.8, corresponding to (2 2 0), (3 1 1), (4 0 0), (4 2 2), (5 1 1) and (4 4 0) planes (blue line in Figure 2b), confirming the presence of γ- Fe_2O_3 phase (Shaoo et al., 2010). In addition to the ruthenium spectra already mentioned above, three extra peaks exist at 2Θ = 82.28, 84.73 and 86.01, corresponding to (2 0 0), (1 1 2) and (2 0 1) planes, respectively (black line in Figure 2b). Ru-Fe was not detected by XRD but was confirmed through Energy Dispersive X-ray (EDX) analysis on both Al_2O_3 and CNTs supports as shown in Figure 3a and 3b, respectively.

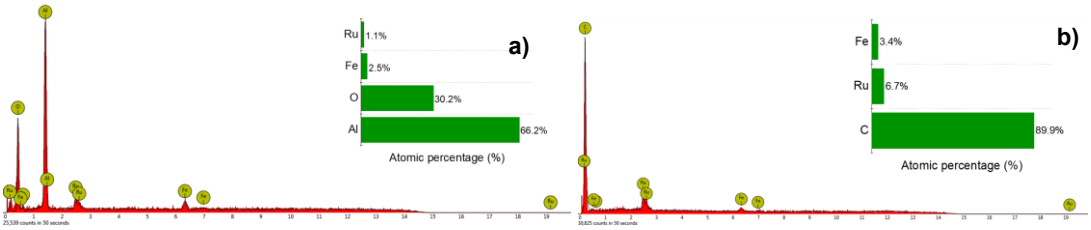

Figure 3: EDX pattern for Ruthenium-Iron on a) Al_2O_3 and b) CNTs with Atomic percentage of metals.

3.2 N_2 Reduction tests

The Al_2O_3 and CNTs-based electrodes were tested in the gas-phase system. Before testing, a rigid electrochemical protocol was performed, consisting of i) decontamination process and ii) a chrono-amperometry (CA) at the desired set potential. The investigated potentials range from -0.1 to -0.8 V vs. RHE. The selection of potential increments was based on preliminary tests, in order to operate at optimal current densities from -100 to -400 μA cm^{-2}, which is the range where the onset potential of the reaction occurs, just before the hydrogen evolution reaction (HER) becomes predominant. The decontamination process was conducted by applying a low potential (-0.1 V vs RHE) for a duration of 60 minutes. This procedure was essential for the removal of any nitrogen contamination (e.g., ammonia or other N-compounds adhered to the electrode surface during deposition or adsorbed to the Nafion membrane) not originating from the nitrogen present in the reactant gas. Furthermore, before testing, the electrolyte and the sulphuric acid trap were subjected to analysis using the spectrophotometric method and the ion chromatograph, respectively. These analyses were performed to ensure the absence of ammonium. The entire apparatus employed for the experiment maintained a gas-tight

environment and the decontamination values have been voluntarily omitted for simplicity. The purpose of this work is to evaluate the option of partial or total replacement of noble metals with more earth-abundant materials. Figures 4a and 4b show the production of ammonia expressed in μg mg_{cat}^{-1} h^{-1} for Al_2O_3 and CNTs-based electrodes, respectively, at different applied potentials. During the tests no ammonia was detected in liquid phase (anodic compartment), and the totality of reduced nitrogen was detected in the gas phase trap (cathode).

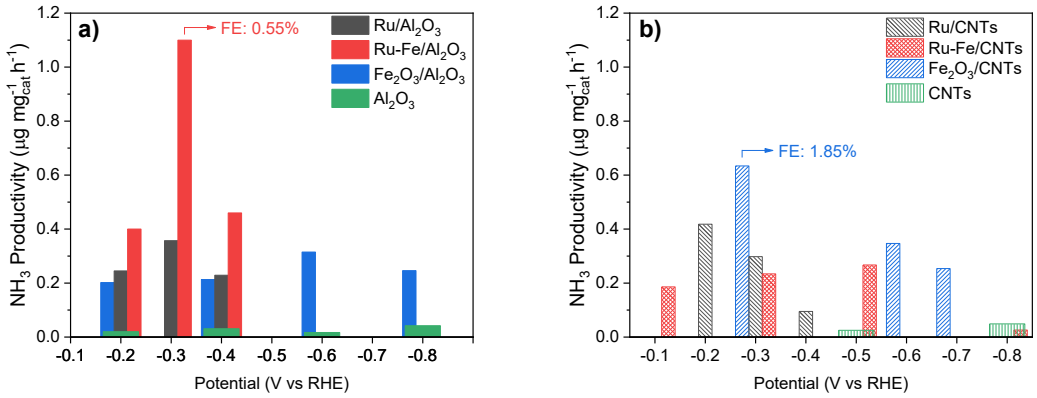

Figure 4: Ammonia production for a) Al_2O_3-based catalysts and b) for CNTs-based catalysts.

The results shown in Figure 4a for alumina-based catalysts denote a predominantly best performance in gas-phase, in terms of ammonia productivity at -0.3 V vs. RHE with the co-doped catalyst Ru-Fe/Al_2O_3, yielded the highest observed catalytic performance (1.16 μg mg_{cat}^{-1} h^{-1}) with a Faradaic Efficiency (FE) of 0.55% and a current density of -294 μA cm^{-2} at -0.3 V vs. RHE. In Figure 4b for functionalized-CNTs-based catalysts, Fe_2O_3/CNTs shows the best performance of 0.62 μg mg_{cat}^{-1} h^{-1} with a FE of 1.5% and a current density of -40 μA cm^{-2} at -0.3 V vs. RHE. Productivity in Ru-Fe co-doped alumina catalyst is 1.87 times more than Iron (III) oxide on CNTs. The presence of ruthenium reduces the onset potential, while iron enhances productivity. In the case of alumina, the partial substitution results in beneficial effects on productivity and the main values for produced ammonia are reported in table 1.

Table 1: Comparison of the best catalyst results for electrochemical approach

Catalysts	NH_3 Productivity (μg mg_{cat}^{-1} h^{-1})	Faradaic Efficiency (%)
Ru-Fe / Al_2O_3	1.16	0.55
Fe_2O_3 / CNTs	0.62	1.85

As reported by Chen et al. (2020), the application of a low potential can change the structure of the active site by forming the active species γ-FeOOH (Lepidocrocite) from γ-Fe_2O_3 phase found in XRD characterization. The active γ-FeOOH is able to promote the reaction in agreement also with the example found in nature with Nitrogenase FeMo-cofactor (Einsle, 2014). Moreover Liu et al. (2023) observed a similar behaviour with Fe-Ru bimetallic catalyst prepared by atomically dispersing the metals on Metal Organic Frameworks (MOFs) by wetness incipient impregnation. When comparing the adsorption and desorption energies by DFT calculations, the presence of atomically dispersed Fe and Ru reduces the N_2-Fe reaction path by reducing the adsorption/desorption energies without being detected by XRD analysis. These results emphasize the need for further research to reach industrial competitiveness and highlight the key role of electrode and reactor engineering in this advancement (Rouwenhorst et al., 2021). The electrochemical NRR future efforts should be addressed to i) increase the maximum productivity compared to the state of the art, ii) increase the mechanical and chemical stability of the catalysts over time, iii) increase the energy efficiency of the process, vi) reduce the use of critical materials having priority for sustainability. Also, the use of a different reaction media such as organic environment (Ampelli, 2020) or ionic liquid (Tian et al., 2022) minimizing the proton activity respect to aqueous media, could reduce the side reaction of HER. Only by incorporating innovative technologies and methodologies, new paths can be opened for substantial improvements in the NRR driven by renewable electricity.

4. Conclusions

The electrocatalytic behaviour of Ru and/or Fe-doped alumina (Al_2O_3) or carbon nanotubes (CNTs) was evaluated in the Nitrogen Reduction Reaction (NRR) in combination with a gas-diffusion layer (GDL) to form novel gas-diffusion electrodes, using custom reactors of advanced design, working in gas phase (i.e. electrolyte-less conditions) to overcome the low solubility of nitrogen in aqueous media. In the case of catalysts based on carbon nanotubes (CNTs), they showed similar activity, such as Fe_2O_3 in comparison to Ru and Ru-Fe co-doped variants. On the contrary, alumina-based catalysts showcased distinctive trends. Specifically, doping with Ru provided higher catalytic performance compared to Fe_2O_3, while the substitution of Fe with Ru in a co-doped configuration (Ru-Fe/Al_2O_3) yielded the highest observed catalytic performance of 1.16 $\mu g\ mg_{cat}^{-1}\ h^{-1}$, and a current density of -294 $\mu A\ cm^{-2}$ at -0.3 V vs RHE. It is evident that, partially replacing an expensive metal (such as Ru) with a less expensive one (Fe) brings benefits. Among all the samples, Fe_2O_3/CNTs showed the best performance of 0.62 $\mu g\ mg_{cat}^{-1}\ h^{-1}$ and a current density of -40 $\mu A\ cm^{-2}$ at -0.3 V vs RHE. Although H_2 is the predominant product observed in these experiments, this study has provided insights into the potential range in which NRR occurs in relation to the electrocatalyst used. Ongoing research aims to reduce H_2 production in favour of NRR by engineering the electrode to modulate wettability properties, thereby controlling proton accessibility to the catalytic active sites.

Acknowledgments

This work was funded by the European Union - Next Generation EU, Mission 4 Component 1 CUP J53D23007700006 through the PRIN 2022 Project HYDREAM (ID: 2022YXHXH5), which is gratefully acknowledged.

References

Ampelli, C., 2020, Electrode design for ammonia synthesis, Nature Catalysis, 3(5), 420–421.

Chen, S., Perathoner, S., Ampelli, C., Mebrahtu, C., Su, D. and Centi, G., 2017, Room-Temperature Electrocatalytic Synthesis of NH_3 from H_2O and N_2 in a Gas–Liquid–Solid Three-Phase Reactor, ACS Sustainable Chemistry & Engineering, 5(8), 7393–7400.

Chen, S., Perathoner, S., Ampelli, C., Wei, H., Abate, S., Zhang, B. and Centi, G., 2020, Enhanced performance in the direct electrocatalytic synthesis of ammonia from N_2 and H_2O by an in-situ electrochemical activation of CNT-supported iron oxide nanoparticles, Journal of Energy Chemistry, 49, 22–32.

Einsle, O., 2014, Nitrogenase FeMo cofactor: an atomic structure in three simple steps, JBIC Journal of Biological Inorganic Chemistry, 19(6), 737–745.

Giusi, D., Miceli, M., Genovese, C., Centi, G., Perathoner, S. and Ampelli, C., 2022, ,In situ electrochemical characterization of Cu_xO-based gas-diffusion electrodes (GDEs) for CO_2 electrocatalytic reduction in presence and absence of liquid electrolyte and relationship with C_{2+} products formation, Applied Catalysis B: Environmental, 318, 121845.

Guo, X.-X., Du, H., Qu, F. and Li, J., 2019, Recent progress in electrocatalytic nitrogen reduction, Journal of materials chemistry. A, Materials for energy and sustainability, 7(8), 3531–3543.

Hirsch, A. and Vostrowsky, O., 2005, Functionalization of Carbon Nanotubes, Topics in current chemistry, 193–237.

Li, D., Zan, L., Chen, S., Shi, Z.-J., Chen, P., Xi, Z. and Deng, D., 2022, Direct conversion of N_2 and O_2: status, challenge, and perspective, National Science Review, 9(12), 2095-5138.

Liu, M., Zhang, S., Chen, M., Zhou, S. and Wu, L., 2023, An isolated bimetallic Fe–Ru single-atom catalyst for efficient electrochemical nitrogen reduction, Journal of Materials Chemistry A, 11(27), 14900–14910.

Park, J., Ko, Y. J., Lim, C., Kim, H., Min, B. K., Lee, K. Y., Koh, J. H., Oh, H. S., & Lee, W. H., 2023, Strategies for CO_2 electroreduction in cation exchange membrane electrode assembly, Chemical Engineering Journal, 453, 139826–139826.

Rafiqul, I., Weber, C., Lehmann, B. and Voss, A., 2005, Energy efficiency improvements in ammonia production—perspectives and uncertainties, Energy, 30(13), 2487–2504.

Rouwenhorst, K.H.R., Krzywda, P.M., Benes, N.E., Mul, G. and Lefferts, L., 2021, Ammonia Production Technologies, Techno-Economic Challenges of Green Ammonia as an Energy Vector, 41–83.

Sahoo, S. K., Agarwal, K., Singh, A. K., Polke, B. G., and Raha, K. C., 2011, Characterization of γ- and α-Fe_2O_3 nano powders synthesized by emulsion precipitation-calcination route and rheological behaviour of α-Fe_2O_3, International Journal of Engineering, Science and Technology, 2(8).

Schrock, R.R., 2006, Reduction of dinitrogen, Proceedings of the National Academy of Sciences, 103(46), 17087–17087

Tavella, F., Giusi, D. and Ampelli, C., 2022, Nitrogen reduction reaction to ammonia at ambient conditions: A short review analysis of the critical factors limiting electrocatalytic performance, Current Opinion in Green and Sustainable Chemistry, 35, 100604.

Tian, Y., Liu, Y., Wang, H., Liu, L. and Hu, W., 2022, Electrocatalytic Reduction of Nitrogen to Ammonia in Ionic Liquids, ACS Sustainable Chemistry & Engineering, 10(14), 4345–4358.